CENTRAL ASIAN JOURNAL OF MEDICAL AND NATURAL SCIENCES
https://cajmns.centralasianstudies.org/index.php/CAJMNS
Volume: 07 Issue: 03 | July 2026 ISSN: 2660-4159

Article

Enhance Formation of Hydroxyapatite and Corrosion Behavior Of Ti13Nb13Zr Alloy Coated with Sio2, Batio3 and Sio2 -Batio3 Composite Comparative Study

Shanai M. Al-Bayati[1], Hamzah K. Rustam[2]

1. PhD in Prosthodontics College of medical Techniques University of AL-Kitab
2. MSc. In prosthodontic ministry of health, specialist dental center in Kirkuk

*Correspondence: Shanai.mohamed@uoalkitab.edu.iq[1], Hamzahdent89@gmail.com[2]

Abstract: Surface modification of titanium alloys is widely employed to improve their bioactivity and corrosion resistance for biomedical implant applications. In this study, Ti-13Nb-13Zr alloy samples were coated with SiO_2, $BaTiO_3$, and a SiO_2–$BaTiO_3$ composite using a spray pyrolysis technique. The coated specimens were immersed in simulated body fluid (SBF) for 30 days to evaluate their apatite-forming ability and bioactivity. The formation of hydroxyapatite and surface characteristics were investigated using X-ray diffraction (XRD), energy-dispersive X-ray spectroscopy (EDX), and field-emission scanning electron microscopy (FESEM). Electrochemical performance was assessed through open-circuit potential (OCP), potentiodynamic polarization, and electrochemical impedance spectroscopy (EIS). The results revealed successful hydroxyapatite formation on all coated surfaces, with the SiO_2–$BaTiO_3$ composite coating exhibiting the highest apatite-forming ability, as evidenced by increased hydroxyapatite peak intensity and a dense surface morphology. Electrochemical measurements demonstrated a significant improvement in corrosion resistance, with the composite-coated sample showing the lowest corrosion rate (1.883×10^{-5} mm·y^{-1}), a protection efficiency of 99.49%, and the highest impedance resistance after SBF immersion. The enhanced performance was attributed to the synergistic effect of SiO_2 and $BaTiO_3$, which promoted hydroxyapatite deposition and improved surface protection. These findings suggest that SiO_2–$BaTiO_3$ composite coatings deposited by spray pyrolysis are a promising surface modification approach for improving the bioactivity and corrosion resistance of Ti-13Nb-13Zr alloy used in biomedical implants.

Keywords: Ti-13Nb-13Zr alloy; SiO_2–$BaTiO_3$ composite coating; Spray pyrolysis; Hydroxyapatite formation; Corrosion resistance; Simulated body fluid; Biomedical implants.

Citation: Al-Bayati S. M., Rustam H. K. Enhance Formation of Hydroxyapatite and Corrosion Behavior Of Ti13Nb13Zr Alloy Coated with Sio2, Batio3 and Sio2 -Batio3 Composite Comparative Study. Central Asian Journal of Medical and Natural Science 2026, 7(3), 668-681.

Received: 10th Mar 2026
Revised: 11th Apr 2026
Accepted: 19th May 2026
Published: 23th Jun 2026

Introduction

The hyydroxyapatite ($Ca_{10}(PO_4)_6(OH)_2$) is an essential component of bone structure; together with collagen, they form the basis for bone formation and structure as shown in fig (1) . Therefore, researchers have been studying how bone forms, especially in fluids similar to body fluids which they call simulated body fluid (SBF). Another studies have shown that the biomimetic formation of hydroxyapatite in the simulated body fluid is greatly affected by the surface on which it begins to form [1]. Titanium alloys were among the most commonly used alloys for manufacturing surgical implants especially Ti13Nb13Zr alloy . Numerous studies have addressed the coating of titanium alloys in

general with various bioceramic materials to accelerate bone growth. These bioceramics such as barium titanate $BaTiO_3$ and silicon dioxide SiO_2 have been the focus of these researches due to their role in accelerating bone growth [2]. Barium titanate ($BaTiO_3$) is a promising, lead-free piezoelectric ceramic heavily researched for advanced bone tissue engineering**.** It mimics the natural piezoelectricity of bone, enabling electrical microenvironments that actively promote cell growth**,** osteogenesis, and wound. Silicon dioxide (SiO_2), or silica, is highly versatile in biomedicine particularly in the form of bioglass. It is prized for its excellent biocompatibility, tunable pore size, large surface area, and ability to release silicate ions that promote bone regeneration [3]. For these characteristics our research we coat Ti13Nb13Zr alloy samples with SiO2, BaTiO3 as individual and together as mix using pyrolysis spray coating and investigate how that coating affect the formation of hydroxyapatite after immersing in simulated body fluid for one month. XRD, EDX X, FESEM and electrochemical corrosion test was achieved to evaluate the results of these samples [4].

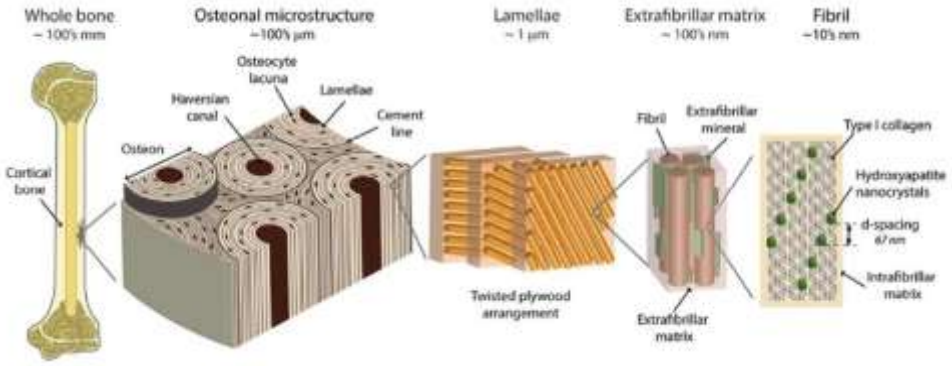

Figure 1. The hierarchical organization of cortical bone.

Materials and Methods

The samples were prepared by cutting Ti13NB13Zr 20mm diameter rod with chemical composition listed in table (1) to 2mm thickness samples using wire cutting machine (DK-7735, China). The samples was grinded using grinding paper (p 120-400) grit and cleaned with acetone (Sigma Aldrich, USA) twice using ultrasonic cleaner bath(Camel FSF030s, China). The coating suspension was prepared by dissolving 1 gm from polyvinylpyrolidone (PVP K30, CDH, India) in 10 ml water and stirred vigorously for 20 minutes using hot plate with magnetic stirrer (Alfa HS 860 , Iran). Follow that step 40 ml of absolute ethanol was added and stirred gently for 10 minutes using hot plate with magnetic stirrer. Then 3 gm of SiO_2 (<30nm, Skyspring Nanomaterial, USA) was added to the previous solution and mixed gently for 10 minutes using hot plate with magnetic stirrer. In order to coating the samples we used spray gun connected to (5 psi pressure) air compressor with 0.1 mm diameter nozzle and spray the suspension from 10 cm distance after preheating the samples to 80 °C on hot plate as shown in fig (2). The coated procedure was repeated to achieve two coated layers, then the samples were heat treated at 100 °C for one hour under air atmosphere using oven (Silver cryst, Germany). Also second and third groups of Ti13NB13Zr alloy 2 mm thickness samples was coated with $BaTiO_3$ (<40nm, Skyspring Nanomaterial, USA) and mixed composite from SiO_2 and $BaTiO_3$with 50% of each one by using the same previous procedure of preparing composite solution and coating. The samples the in immersed in synthetic simulated body fluid (SBF) for one month. The SBF solution eas prepared by mixing the chemical component in table (1) in one liter of deionized water and mixed vigorously for 30 minutes using hot plate with magnetic stirrer. The pH of the SBF solution was adjusted to pH= 7.2 using pH meter (Hanna Instruments, HI2210, Germany) by adding diluted hydrochloric acid or diluted sodium hydroxide as required. The immersed samples were heat treated at 100°C in oven

for one hour under air atmosphere. The immersed samples were tested by XRD ,EDX and FESEM, then electrochemical corrosion test also achieved by testing OCP, polarization curve tafel, and electrochemical impedance spectroscopy EIS using potentiostat (CHI 604E, CHINA). The sample was connected as the working electrode, the graphite electrode as the counter electrode, and Ag/AgCl/KCl 3.5M electrode as the reference electrodes as shown in fig (3), while the corrosion media was (SBF) solution.

Table 1. chemical composition of Ti13Nb13ZR alloy.

Chemical composition [% wt.]							
Nb	**Zr**	**Fe**	**C**	**H**	**O**	**S**	**Ti**
13.18	**13.49**	**0.085**	**0.035**	**0.004**	**0.078**	**<0.001**	**balanced**

Table 2. chemical composition of simulated body fluid (SBF) solution.

ITEM	Reagent	Concentration g/l
1	**8.035**	**NaCl**
2	**0.355**	**$NaHCO_3$**
3	**0.225**	**KCl**
4	**0.231**	**K_2HPO_4**
5	**0.311**	**$MgCl_2.6H_2O$**
6	**0.292**	**$CaCl_2$**
7	**0.072**	**Na_2SO_4**

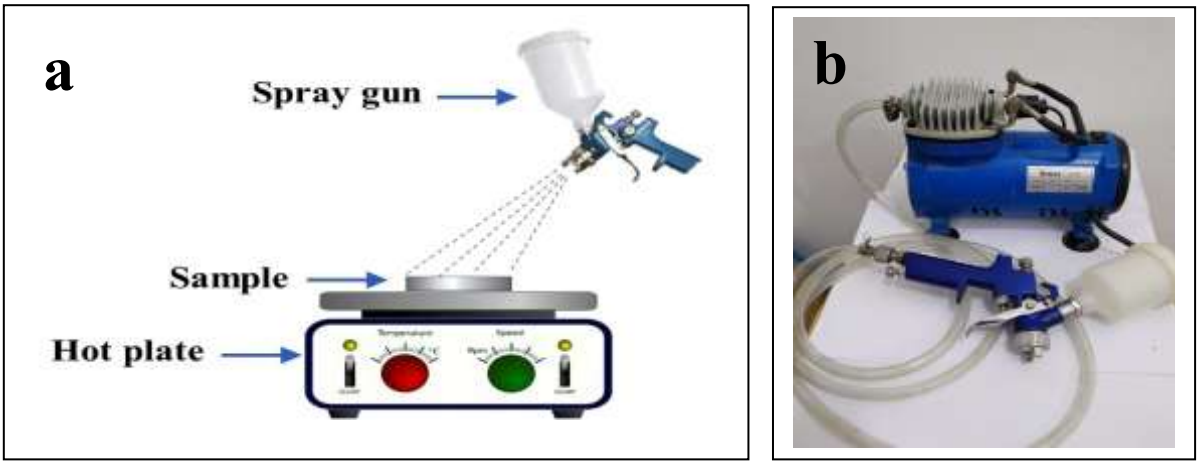

Figure 2. A: Simplified diagram for pyrolysis spray coating process, B: The pyrolysis spray system.

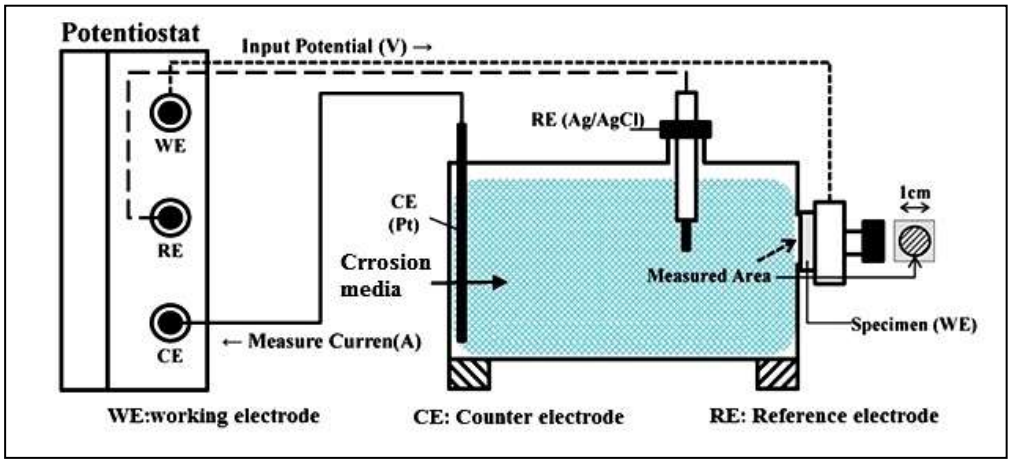

Figure 3. Schematic diagram for sample connection to the potentiostat for corrosion test.

Results

1-XRD Test:

The XRD pattern for Ti13Nb13Zr alloy uncoated sample in fig (4) shows the appearance of hydroxapatite peaks matching JCPDS standard card 00-009-0432 for hydroxyapatite after immersing in SBF solution and four peaks for titanium matching with JCPDS no. 00-044-1294 for titanium. The appearance of titanium peaks was an indicator for poor covering the sample surface with hydroxyapatite [5].

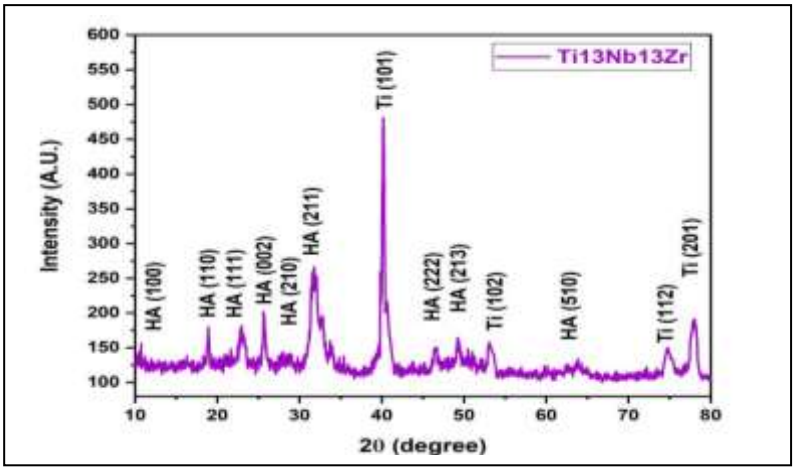

Figure 4. XRD pattern for Ti13Nb13Zr alloy uncoated sample.

The XRD pattern for sample coated with SiO_2 nanopowder in fig (5) shows obviously the appearance of hydroxapatite peaks matching JCPDS standard card 00-009-0432 for hydroxyapatite. Only one peaks appeared matching with JCPDS no. 00-040-1498 for SiO_2 and no titanium peak was observed in the pattern as indicator that the coating was covered the sample surface [6].

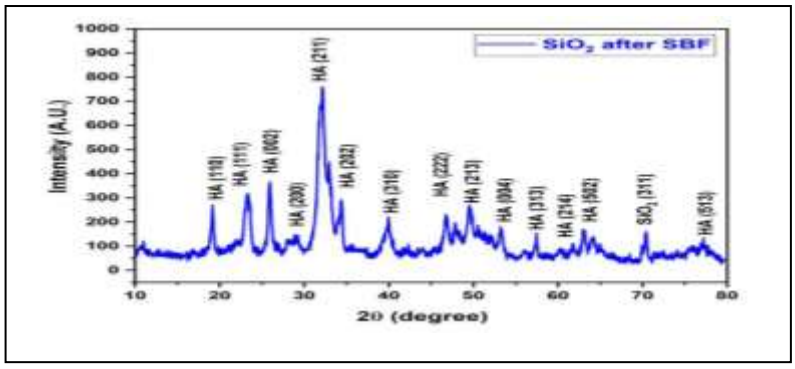

Figure 5. XRD pattern for SiO_2 after immersing in SBF solution for one month.

The XRD pattern for sample coated with $BaTiO_3$ nanopowder in fig (6) shows the appearance of hydroxyapatite peaks matching JCPDS standard card no. 00-009-0432 for hydroxyapatite and appearance of one peak for $BaTiO_3$ matching JCPDS standard card no.01-075-2116 for $BaTiO_3$ and also no titanium peak was observed in the pattern.

The XRD pattern for sample coated with SiO_2- $BaTiO_3$ mixture composite in fig (7) was also shows the hydroxyapatite peaks matching JCPDS standard card no. 00-009-0432 for hydroxyapatite and only one peaks appeared matching with JCPDS no. 00-040-1498 for SiO_2 and one peak observed for $BaTiO_3$ matching JCPDS standard card no.01-075-2116 for $BaTiO_3$. Also no titanium peak was observed in the pattern [7].

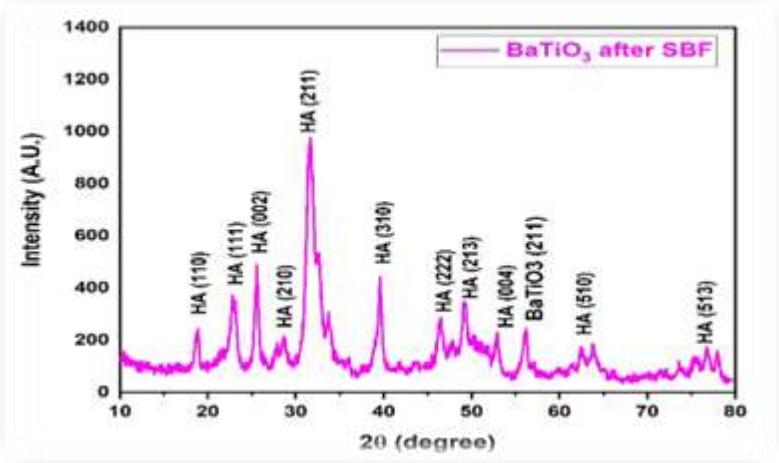

Fiigure 6. Fig (5) XRD pattern for $BaTiO_3$ after immersing in SBF solution for one month.

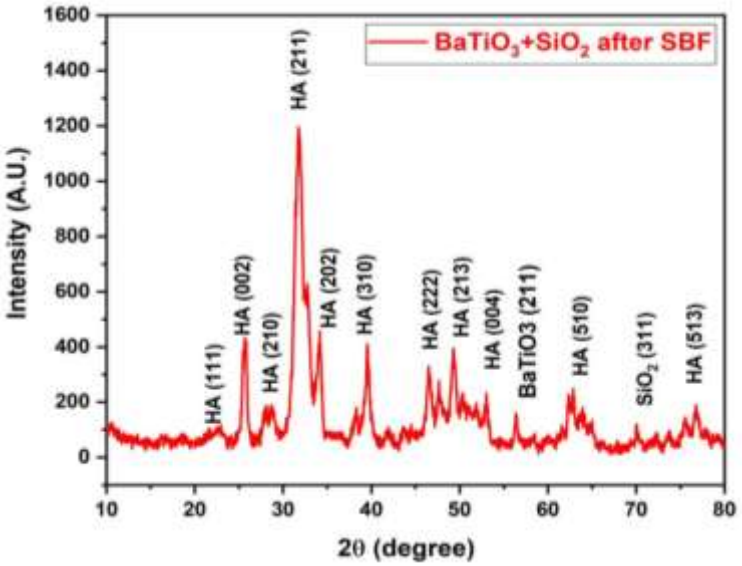

Figure 7. XRD pattern for SiO_2-$BaTiO_3$ mixture composite after immersing in SBF solution for one month.

Fig (8) shows the comparison for all coated samples. We see obviously the increasing in peaks intensity gradually from uncoated sample until that coated with SiO_2-$BaTiO_3$ mixture composite. Where that arrangement of increasing in intensity was uncoated base, SiO_2, $BaTiO_3$ and SiO_2-$BaTiO_3$ mixture composite. This indicate was the final sample was more biocompatible and has more ability to attract the hydroxyapatite and make it more grown over the sample surface, i.e. it has more osseointegration ability [8].

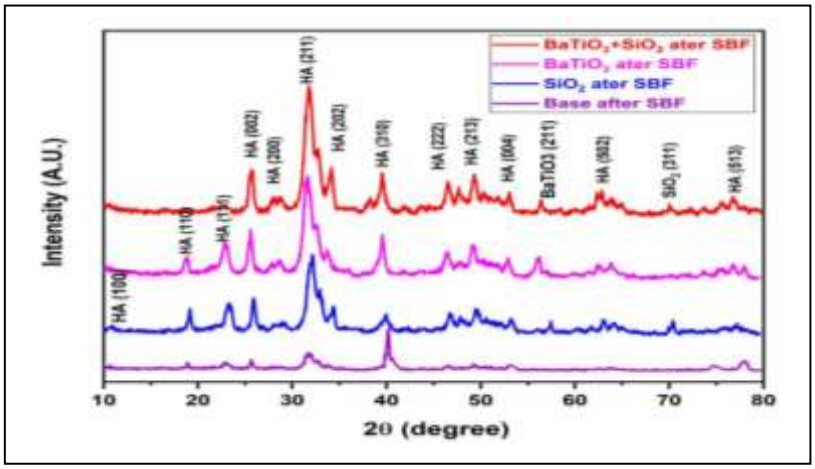

Figure 8. the XRD pattern comparison for all coated samples.

2-EDX test:

The EDX elemental analysis for uncoated alloy after immersing in SBF solution in fig (9) shows the appearance of calcium phosphorus and magnesium as indicator for hydroxyapatite formation. Also the appearance of titanium refers to high porous and uncovered sample surface with hydroxyapatite.

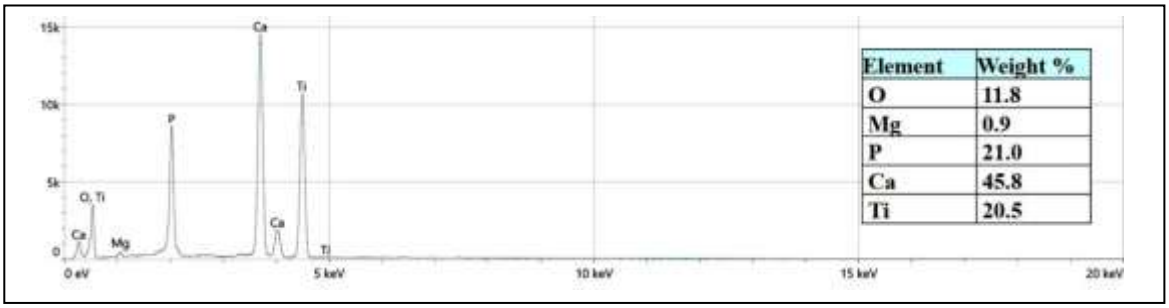

Element	Weight %
O	11.8
Mg	0.9
P	21.0
Ca	45.8
Ti	20.5

Figure 9. EDX elemental analysis for uncoated alloy after immersing in SBF solution.

The ratio of calcium to the phosphorus in natural hydroxyapatite ($Ca_{10}(PO_4)_6(OH)_2$) known as 1.6667 as atomic ratio, so we can be calculate it as weight percent ratio as below:

Ca/P = (10 ×Ca Mwt.)/(6× P Mwt.)

Where Ca Mwt. = calcium molecular weight and P Mwt. = phosphorus molecular weight

(10 × 40.078) / (6×30.9737) = 2.1565

From EDX elemental analysis the Ca/P ratio for the hydroxyapatite formed from SBF solution was equal to 2.180 and it's very close to that for natural hydroxyapatite [9].

The EDX elemental analysis for sample coated with SiO_2 after immersing in SBF solution in fig (10) shows the appearance of calcium phosphorus, magnesium and sodium came from natural formation of hydroxyapatite. Also we see the appendence of silicone came from SiO_2. There was no appearance of titanium or any element from base alloy, i.e. the covering of coating with SiO_2 and the natural formed hydroxyapatite cover the sample surface very well. The Ca/P ratio was 2.171 and it's also very close to that for natural hydroxyapatite [10].

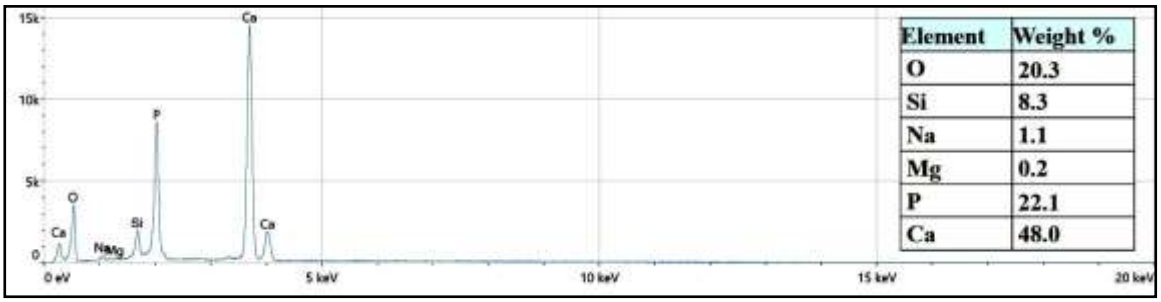

Figure 10. EDX elemental analysis for sample coated with SiO_2 after immersing in SBF solution.

The EDX elemental analysis for sample coated with $BaTiO_3$ after immersing in SBF solution in fig (11) shows the appearance of same elements as previous sample for same reason but with the appendance of barium and titanium came from $BaTiO_3$. The Ca/P ratio was 2.172 near to that for natural hydroxyapatite.

The EDX elemental analysis for sample coated with SiO_2 and $BaTiO_3$ mixture composite after immersing in SBF solution in fig (12) shows the appearance of the elements calcium phosphorus, magnesium and sodium came from hydroxyapatite formation beside silicone, barium and titanium came from SiO_2 and $BaTiO_3$ mixture. The Ca/P ratio was 2.182 near to that for natural hydroxyapatite.

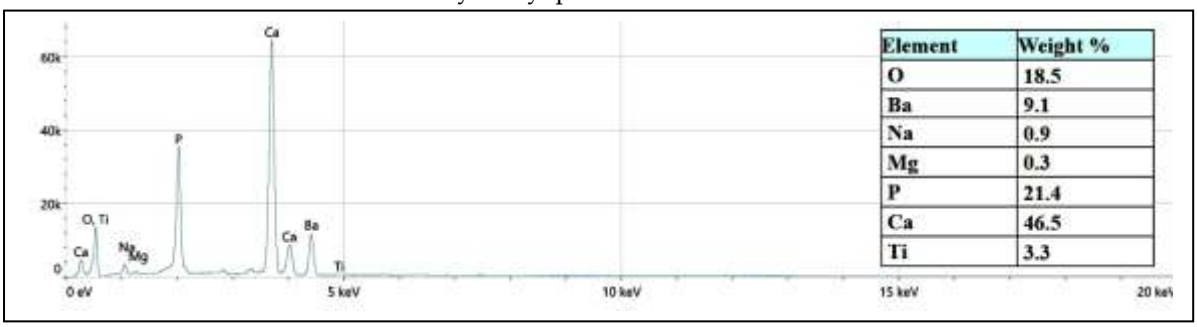

Figure 11. EDX elemental analysis for sample coated with $BaTiO_3$ after immersing in SBF solution.

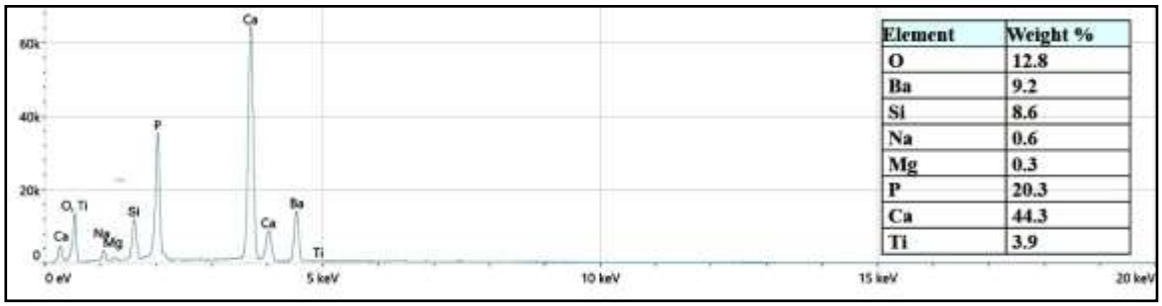

Figure 12. Fig (11) EDX elemental analysis for sample coated withSiO_2 and $BaTiO_3$ mixture after immersing in SBF solution.

3-FESEM test:

The FESEM test images for uncoated sample after immersing in SBF solution in fig (13 a and b) shows formation of hydroxyapatite on the sample surface where the shape of hydroxyapatite varied between agglomerated particles and flakes. The particle size varied between 62.49 to 98.72 nm.

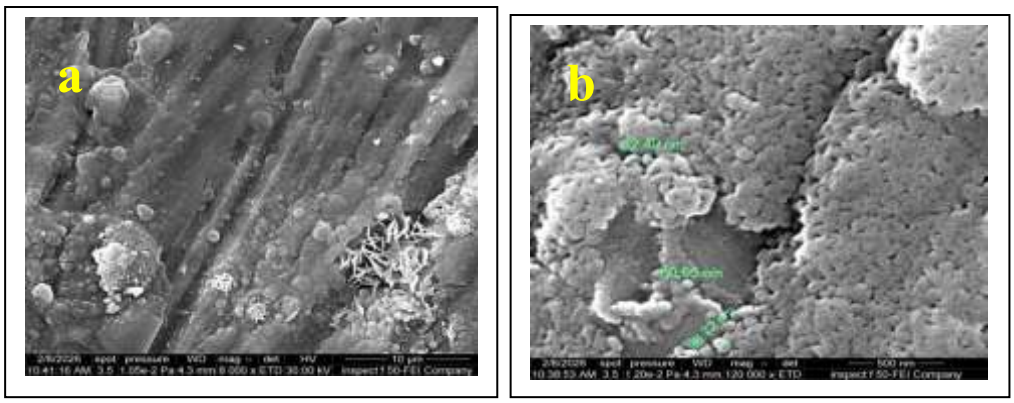

Figure 13. FESEM images for uncoated sample after immersing in SBF solution in different magnification [11].

Discussion

The FESEM images for samples coated with SiO_2,$BaTiO_3$ and SiO_2-$BaTiO_3$ mixture in fig (14 a-f) shows very thick porous layer of hydroxyapatite formed from SBF solution.

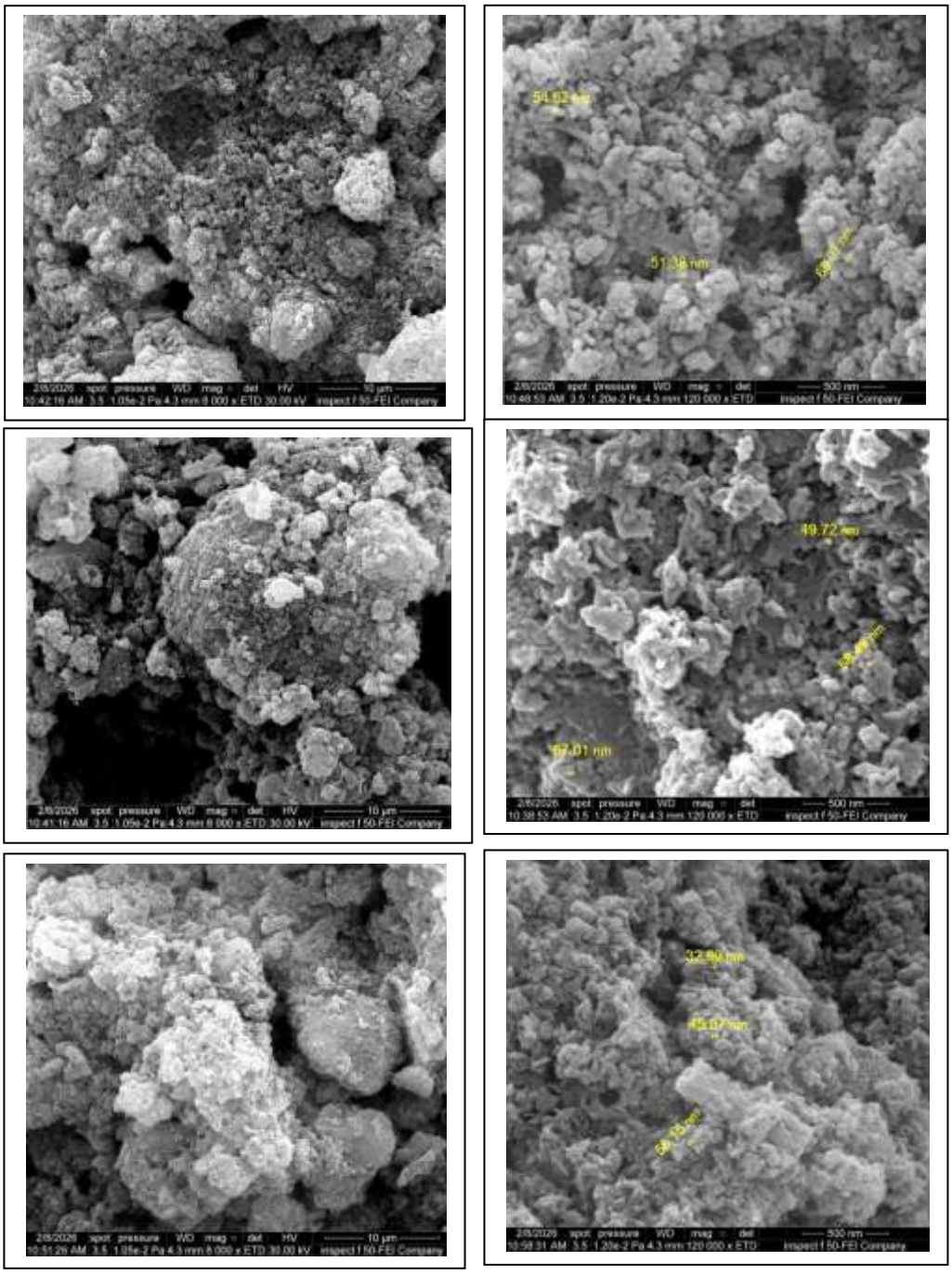

Figure 14. FESEM test images with different magnification for samples coated with (a ,b): SiO_2, (c,d): $BaTiO_3$, (E,F): SiO_2-$BaTiO_3$ mixture.

The FESEM test images for sample coated with SiO_2-$BaTiO_3$ mixture shows more agglomeration than that coated with $BaTiO_3$ and SiO_2 subsequently. The particle size for hydroxyapatite varied between 32.89 to 68.07 nm.

4- Electrochemical corrosion test:

Open circuit potential (OCP) TEST:

The OCP test shows gradually increasing in passivation from uncoated sample to that coated with SiO_2-$BaTiO_3$ mixture. Where the last one achieved 0.025 V compared with -0.655 for uncoated one before immersing [12].

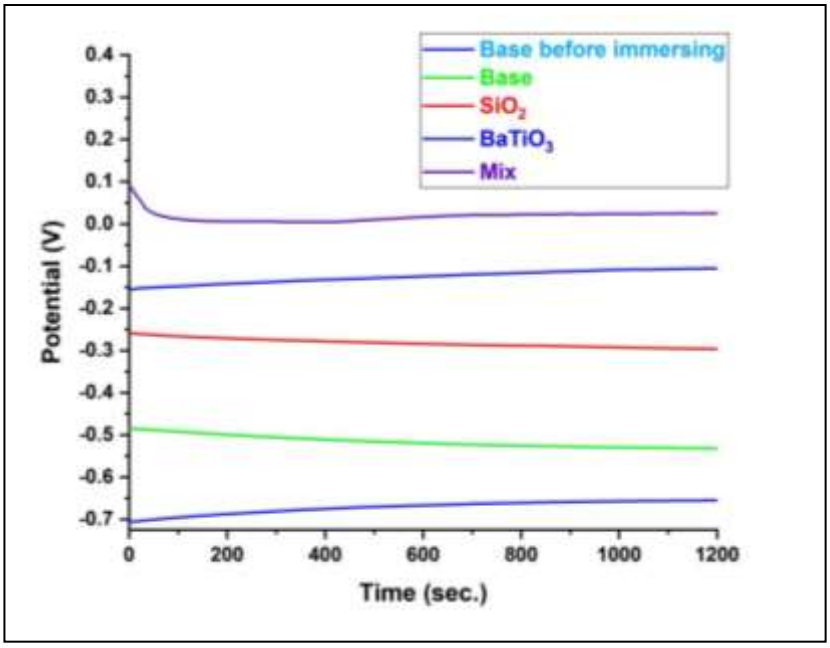

Figure 15. OCP test for all samples.

Table 3. OCP test results for all samples.

ITEM	OCP (volt)
Base before SBF	-0.655
Base	-0.531
SiO_2	0.296-
$BaTiO_3$	-0.105
MIX	0.025

Polarization curve (tafel) test:

The polarization curve comparison for all samples in fig (16) and table (4) shows decreasing in corrosion rate for sample coated with SiO_2-$BaTiO_3$ mixture more than the others, where it was achieve 1.883×10^{-5} mmpy compared with 3.716×10^{-3} mmpy for uncoated sample, i.e. the corrosion rate decreased about 197 times.

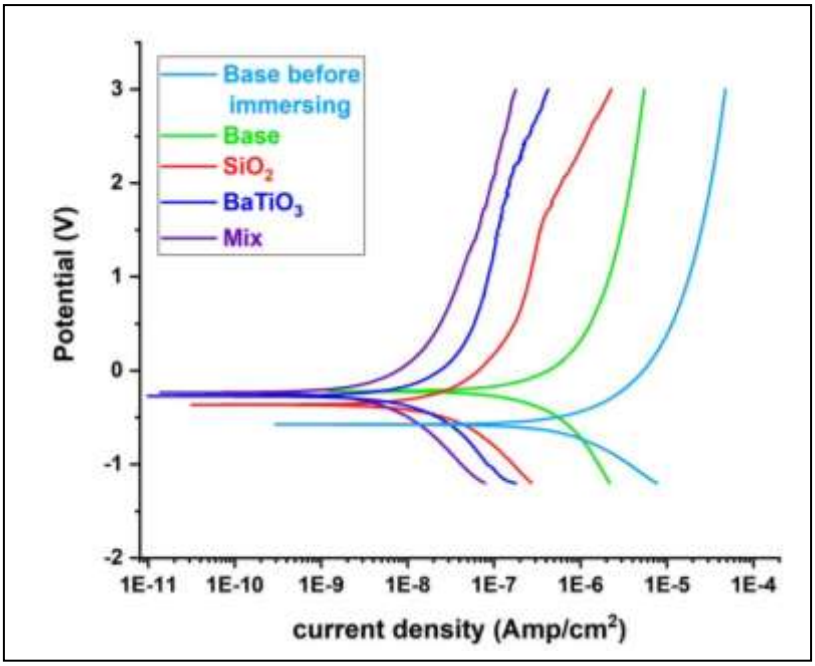

Figure 16. Polarization curve comparison for all samples.

Table 4. Parameters extracted from polarization curve (tafel) for all samples.

ITEM	Ecorr. (volt)	Icorr. (Amp)	Corr. Rate (mmpy)
Base before SBF	-0.556	4.224×10^{-7}	3.716×10^{-3}
Base	-0.219	8.590×10^{-8}	7.558×10^{-4}
SiO_2	-0.364	8.450×10^{-9}	7.435×10^{-5}
$BaTiO_3$	-0.258	4.212×10^{-9}	3.706×10^{-5}
MIX	-0.241	2.140×10^{-9}	1.883×10^{-5}

We can calculate the protection efficiency from the relation below:

$$PE\% = \frac{icorr.\ uncoated - icorr.\ coated}{icorr.\ uncoted} \times 100 \ \ldots\ldots.$$

Where *icorr. uncoated*: the corrosion current for uncoated sample after immersing in SBF and *icorr. coated* the corrosion current for coated sample after immersing in SBF.

The calculated protection efficiency in table (5) shows that all samples except uncoated one achieved more than 97% protection efficiency, where the sample coated with SiO_2-$BaTiO_3$ mixture achieved the higher one equal to 99.49%.

Table 5. calculated protection efficiency for all samples.

ITEM	Icorr. (Amp)	protection efficiency %
Base before SBF	4.224×10^{-7}	-------
Base	8.590×10^{-8}	79.63
SiO_2	8.450×10^{-9}	97.99
$BaTiO_3$	4.212×10^{-9}	99.00
Mix	2.140×10^{-9}	99.49

Electrochemical impedance spectroscope (EIS) test:

The EIS test was achieved for optimum sample (coated with SiO_2-$BaTiO_3$ mixture) compared with the un coated base before and after immersing in SBF solution. After fitting the resulting nyquist diagram for all samples we see that the uncoated sample shows a typical randles equivalent circuit before immersing in SBF solution as shown in fig (17 a and b). Also we see the coated sample shows an equivalent circuit for porous layer connected to the boundary double layer as shown in fig (18 a and b). After immersing in SBF solution the base sample shows different equivalent circuit for another porous layer formed on the sample surface shown in fig (19 a and b). Also the coated layer shows the formation of new porous layer connected to coated layer in the fitted equivalent circuit as

shown in fig (20 a and b). The comparison of all samples in fig (21) and table (6) shows how the new hydroxyapatite increase the resistance for both samples where the total resistance for uncoted sample increase to 10611 ohm compared with 2713 ohm before immersing, and the coated sample increased to 81348 ohm compared with 26346 ohm after immersing. This happened because the new hydroxyapatite formed layer filled the pores present in the previous SiO_2 and $BaTiO_3$ mixture layer and built another layer on top of it [13].

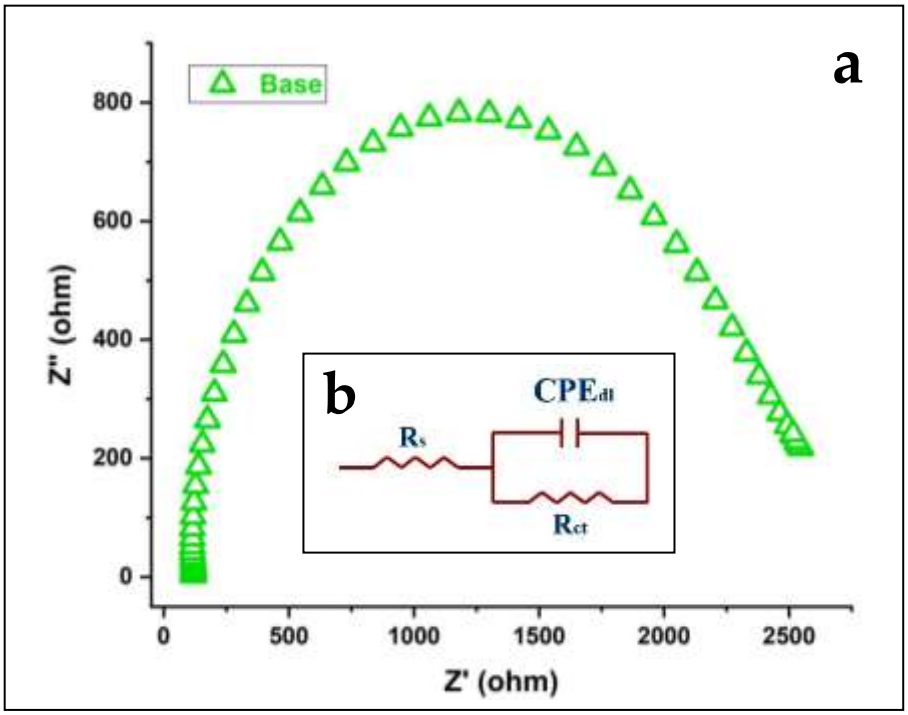

Figure 17. a: nyquist diagram for un coated base sample, b: equivalent circuit used for fitting.

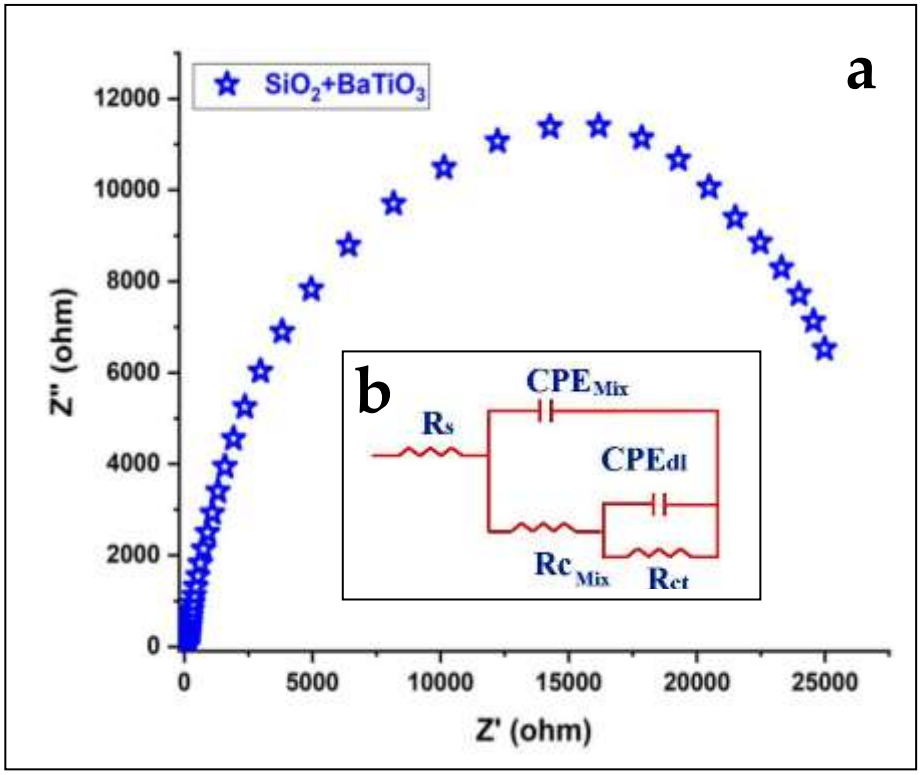

Figure 18. a: nyquist diagram for mixture coated sample, b: equivalent circuit used for fitting.

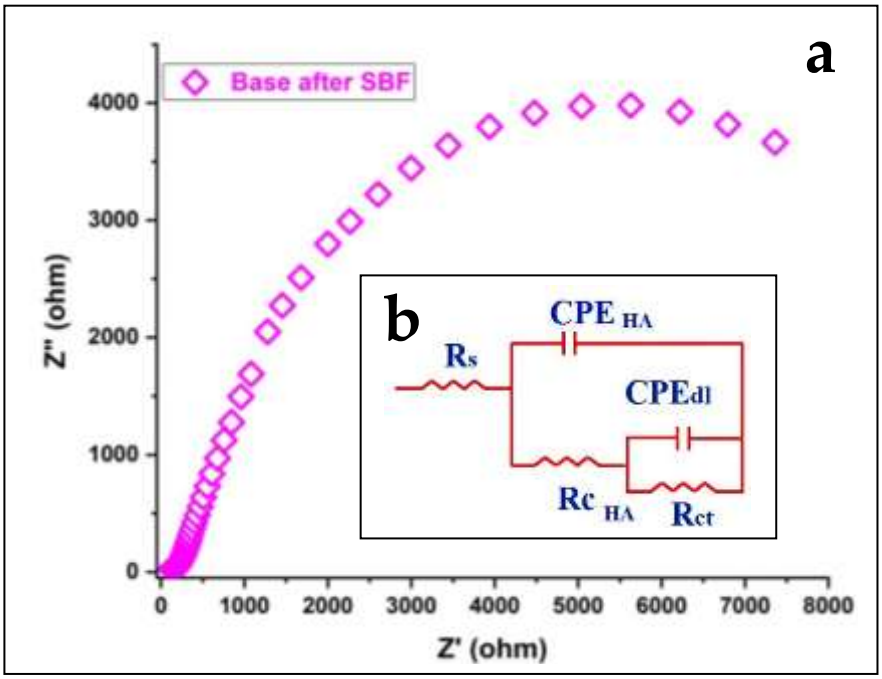

Figure 19. a: nyquist diagram for un coated base sample after immersing in SBF solution, b: equivalent circuit used for fitting.

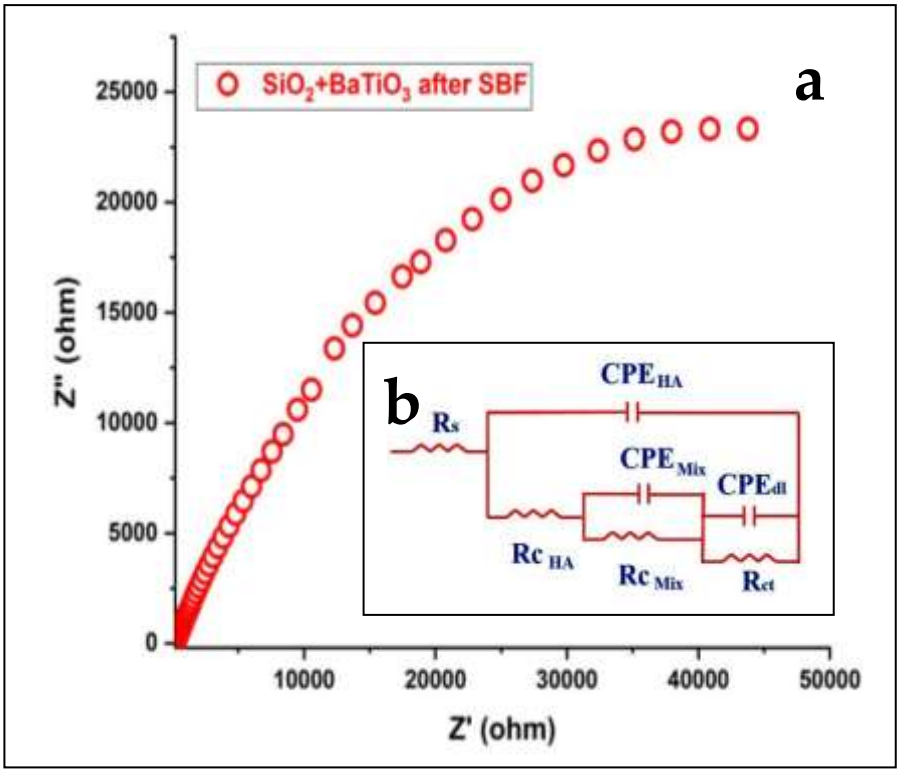

Figure 19. a: nyquist diagram for mixture coated sample after immersing in SBF solution, b: equivalent circuit used for fitting.

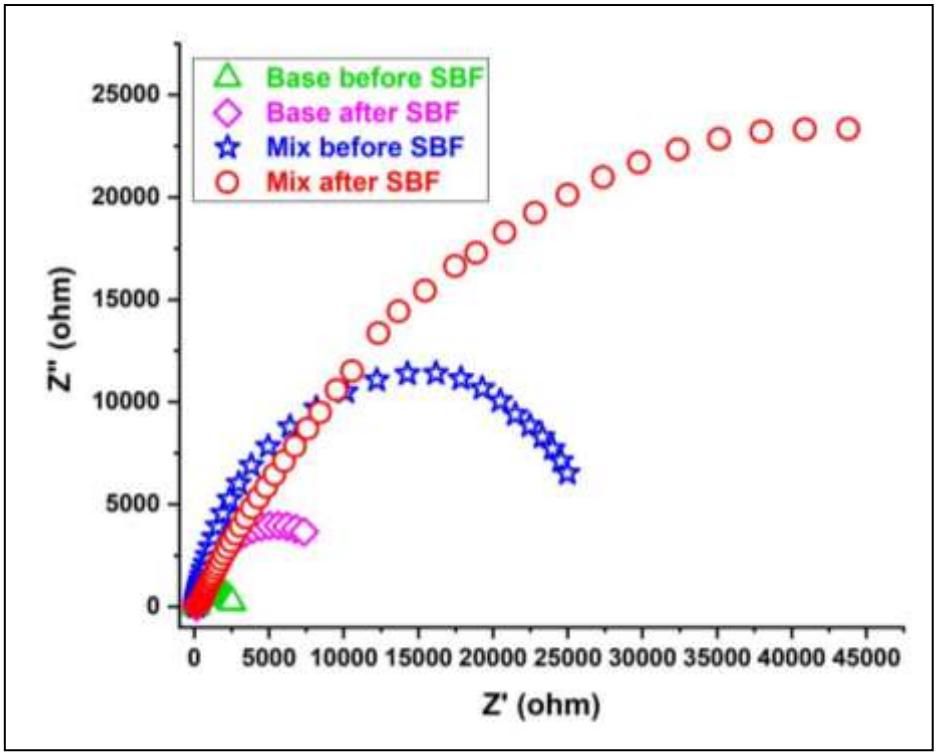

Figure 20. Nyquis diagram comparison for all samples.

Table 6. extracted parameters from fitting the two samples

Parameters	Before immersing in SBF		After immersing in SBF	
	Uncoated	Mix coated	Uncoated	Mix coated
R_S (ohm)	101	98	105	100
R_C(ohm)	-----	23200	-----	8631
R_{CHA}(ohm)	-----	-----	7430	68332
R_{dl}(ohm)	2612	3048	3079	4285
CPE_C(F)	-----	3.7586E-04	----	1.5458E-06
n1	-----	0.997	----	0.919
CPE_{CHA}(F)	-----	-----	2.1418E-05	8.6654E-07
n1	-----	-----	0.915	0.905
CPE_{dl}(F)	3.7221E-06	2.2116E-06	1.7508-04	1.0002E-05
n2	0.96469	0.939	0.994	0.921
Rtotal (ohm)	2713	26346	10614	81348

It is worth noting that the resistance of double layer also increased when hydroxyapatite formed on samples surface and fill the pores, where the for uncoated base sample increased from 2612 ohm to 3079 ohm, and for coated one increased from 3048 ohm to 4285 ohm [14]. This happened because when the hydroxyapatite filled the pores making it more difficult for the oxide layer to leave the sample surface and go to the corrosion media (SBF) so that it be an additional protected layer, the more difficult it becomes for the oxide layer to leave, the higher the resistance becomes, because the oxide continues to form and cannot leave the surface [15].

Conclusion

From previous results we conclude that the coating SiO_2 and $BaTiO^3$ mixture composite was best than coating with each biomaterial alone for the purpose of attracting hydroxyapatite from body fluid solutions and increasing bone formation. The XRD test proves the increasing in hydroxyapatite peaks intensity and FESEM test image shows more agglomeration when coating the sample with previous mixture. The corrosion test proves that the passivation will increase and corrosion rat will decreased about 197 times

than uncoated sample. The EIS test also prove the increasing in resistance after immersing in SBF solution and reach to 81348 ohm compared with 26346 ohm before immersing because theformation of hydroxyapatite which fill the pores of the coated layer and built another layer over it.

REFERENCES

[1] H. Shi, Z. Zhou, W. Li, Yuan Fan, Z. Li, and J. Wei, "Hydroxyapatite based materials for bone tissue engineering: A brief and comprehensive introduction," *Crystals*, vol. 11, no. 2, p. 149, Feb. 2021, doi: 10.3390/cryst11020149.

[2] A. Vercher-Martínez, E. Giner, C. Arango, and F. J. Fuenmayor, "Influence of the mineral staggering on the elastic properties of the mineralized collagen fibril in lamellar bone," *J. Mech. Behav. Biomed. Mater.*, vol. 42, pp. 115–124, Feb. 2015, doi: 10.1016/j.jmbbm.2014.11.009.

[3] N. Beisekenov, M. Sadenova, B. Azamatov, and B. Syrnev, "Analysis of biomechanical characteristics of bone tissues using a Bayesian neural network: A narrative review," *J. Funct. Biomater.*, vol. 16, no. 2, p. 168, 2025, doi: 10.3390/jfb16020168.

[4] O. Kaygili, S. Keser, M. Kom, N. Bulut, and S. V. Dorozhkin, "The effect of simulating body fluid on the structural properties of hydroxyapatite synthesized in the presence of citric acid," *Prog. Biomater.*, vol. 5, no. 3, pp. 173–182, Dec. 2016, doi: 10.1007/s40204-016-0057-x.

[5] W. Dong *et al.*, "Revised method for preparation of simulated body fluid for assessment of the apatite-forming ability of bioactive materials: proposal of mixing two stock solutions," *RSC Adv.*, vol. 14, no. 44, pp. 38660–38667, 2024, doi: 10.1039/D4RA05844E.

[6] P. N. Chavan, M. M. Bahir, R. U. Mene, M. P. Mahabole, and R. S. Khairnar, "Study of nanobiomaterial hydroxyapatite in simulated body fluid: Formation and growth of apatite," *Mater. Sci. Eng. B*, vol. 168, no. 1, pp. 224–230, Apr. 2010, doi: 10.1016/j.mseb.2009.11.018.

[7] E. Nesseri, S. C. Boyatzis, N. Boukos, and G. Panagiaris, "Optimizing the biomimetic synthesis of hydroxyapatite for the consolidation of bone using diammonium phosphate, simulated body fluid, and gelatin," *SN Appl. Sci.*, vol. 2, no. 11, p. 1892, Nov. 2020, doi: 10.1007/s42452-020-03694-x.

[8] M. S. Baltatu, A. V. Sandu, M. Nabialek, P. Vizureanu, and G. Ciobanu, "Biomimetic deposition of hydroxyapatite layer on titanium alloys," *Micromachines*, vol. 12, no. 12, p. 1447, Nov. 2021, doi: 10.3390/mi12121447.

[9] I. V. Pylypchuk, A. L. Petranovska, M. P. Turelyk, and P. P. Gorbyk, "Formation of biomimetic hydroxyapatite coating on titanium plates," *Mater. Sci. (Medžiagotyra)*, vol. 20, no. 3, pp. 314–318, 2014, doi: 10.5755/j01.ms.20.3.4912.

[10] I. V. Pylypchuk, A. L. Petranovska, O. I. Oranska, and P. P. Gorbyk, "Biomimetic hydroxyapatite formation on titanium surface in simulated body fluids of different chemical composition," *Chem. Phys. Technol. Surf.*, vol. 5, no. 4, pp. 415–420, 2014.

[11] G. H. Farhan, J. A. Hassan, and A. H. Al-helli, "Coating Ti13Nb13Zr alloy with hydroxyapatite using pyrolysis spray improves corrosion and osseointegration characteristics for biomedical applications (In-vitro study)," *Prog. Color Colorants Coat.*, vol. 19, no. 2, pp. 113–133, 2026.

[12] S. Sathish, M. Geetha, S. T. Aruna, N. Balaji, K. S. Rajam, and R. Asokamani, "Studies on plasma sprayed bi-layered ceramic coating on bio-medical Ti–13Nb–13Zr alloy," *Ceram. Int.*, vol. 37, no. 4, pp. 1333–1339, May 2011, doi: 10.1016/j.ceramint.2010.12.008.

[13] K. E. Ibrahim and H. A. Kassim, "Hydroxyapatite-modified Mg-doped BaTiO3 composites with improved physical properties for biomedical applications," *Ceram.-Silikaty*, vol. 69, no. 4, pp. 534–542, 2025, doi: 10.13168/cs.2025.0042.

[14] Y. Mochizuki, N. Tsubouchi, and K. Sugawara, "Synthesis of BaTiO3 nanoparticles from TiO2-coated BaCO3 particles derived using a wet-chemical method," *J. Asian Ceram. Soc.*, vol. 2, no. 1, pp. 53–59, Mar. 2014, doi: 10.1016/j.jascer.2014.01.002.

[15] C. Gül, S. Albayrak, H. Durmuş, and N. Çömez, "Characterization of SiO2 sol-gel coated Ti6Al4V alloy obtained by using TEOS and GPTMS," *Sci. Sinter.*, vol. 53, no. 4, pp. 461–473, 2021, doi: 10.2298/SOS2104461G.